British Journal of Pharmacology

DOI:10.1111/j.1476-5381.2010.01115.x
www.brjpharmacol.org

RESEARCH PAPER

Biomechanical properties and innervation of the female caveolin-1-deficient detrusor

Mardjaneh Karbalaei Sadegh[1], Mari Ekman[1], Catarina Rippe[1], Frank Sundler[1], Nils Wierup[1], Michiko Mori[1], Bengt Uvelius[2] and Karl Swärd[1]

[1]*Department of Experimental Medical Science, Lund University, Biomedical Centre, Lund, Sweden, and* [2]*Department of Urology, Clinical Sciences, Lund University, Lund, Sweden*

Correspondence
Dr Karl Swärd, Department of Experimental Medical Science, Lund University, BMC D12, SE-221 84 Lund, Sweden. E-mail: karl.sward@med.lu.se

Keywords
caveolae; carbachol; ATP; purine receptor; CGRP; CART; NPK; synaptophysin; caveolin; cavin; lower urinary tract dysfunction; MuSK

Received
24 June 2010
Revised
7 October 2010
Accepted
19 October 2010

BACKGROUND AND PURPOSE

Caveolin-1-deficiency is associated with substantial urogenital alterations. Here, a mechanical, histological and biochemical characterization of female detrusors from wild-type and caveolin-1-deficient (KO) mice was made to increase the understanding of detrusor changes caused by lack of caveolae.

EXPERIMENTAL APPROACH

Length–tension relationships were generated, and we recorded responses to electrical field stimulation, the muscarinic receptor agonist carbachol and the purinoceptor agonist ATP. Tyrosine nitration and the contents of caveolin-1, cavin-1, muscarinic M_3 receptors, phospholipase $C_{\beta1}$, muscle-specific kinase (MuSK) and L-type Ca^{2+} channels were determined by immunoblotting. Innervation was assessed by immunohistochemistry.

KEY RESULTS

Bladder to body weight ratio was not changed, nor was there any change in the optimum circumference for force development. Depolarization- and ATP-induced stress was reduced, as was carbachol-induced stress between 0.1 and 3 μM, but the supramaximal relative (% K^+) response to carbachol was increased, as was M_3 expression. The scopolamine-sensitive component of the electrical field stimulation response was impaired, and yet bladder nerves contained little caveolin-1. The density of cholinergic nerves was unchanged, whereas CART- and CGRP-positive nerves were reduced. Immunoblotting revealed loss of MuSK.

CONCLUSIONS AND IMPLICATIONS

Ablation of caveolae in the female detrusor leads to generalized impairment of contractility, ruling out prostate hypertrophy as a contributing factor. Cholinergic neuroeffector transmission is impaired without conspicuous changes in the density of cholinergic nerves or morphology of their terminals, but correlating with reduced expression of MuSK.

Abbreviations

CART, cocaine- and amphetamine-regulated transcript; Cav-1 or Cav1, caveolin-1; $Ca_V1.2$, pore-forming subunit of L-type Ca^{2+} channel; CGRP, calcitonin gene-related peptide; EFS, electrical field stimulation; HK, K^+-high solution (60 mM); HTX, Mayer's haematoxylin; KO, caveolin-1 knockout; L_0, optimum circumference for force development; M_3, type 3 muscarinic acetylcholine receptor; MuSK, muscle-specific kinase; NPK, neuropeptide K; $PLC_{\beta1}$, phospholipase $C_{\beta1}$; VAChT, vesicular acetylcholine transporter; WT, wild type

Introduction

Caveolae are Ω-shaped membrane invaginations that are abundant in adipose tissue, endothelia and muscle (Cohen *et al.*, 2004). In smooth muscle cells of the urinary bladder, caveolae are arranged in arrays along the cell axis (Murakumo *et al.*, 1993). Biochemical methods have been used to isolate caveolae and to show that cellular signalling proteins, including tyrosine kinases, phospholipases, receptors and ion channels, are represented in caveola preparations (Lisanti *et al.*,

1994a; Liu *et al.*, 1997; Babiychuk *et al.*, 2004; Absi *et al.*, 2007). Such findings have fuelled the concept that regulated signalling may occur through discrete membrane microdomains (Lisanti *et al.*, 1994b; Taggart, 2001). Caveola biogenesis depends on proteins from the caveolin (Cohen *et al.*, 2004) and cavin (Hill *et al.*, 2008; Bastiani *et al.*, 2009) families and on the content of cholesterol in the cell membrane (Rothberg *et al.*, 1992).

In keeping with the high density of caveolae in the urogenital tract, caveolin-1-deficiency from birth is associated with substantial urogenital alterations in male mice. These changes include prostate and bladder hypertrophy (Woodman *et al.*, 2004), distension of the seminal vesicles (Woodman *et al.*, 2004), disturbed erectile mechanisms (Shakirova *et al.*, 2009), impaired contractility of isolated detrusor strips (Lai *et al.*, 2004; 2007; Woodman *et al.*, 2004) and impaired cholinergic neurotransmission in the detrusor (Lai *et al.*, 2004).

The short-term response to bladder outflow obstruction, such as that caused by prostatic enlargement, involves detrusor growth and denervation (Andersson, 2003). Obstruction also leads to impaired muscarinic contractility (Saito *et al.*, 1993). Thus, the bladder phenotype of caveolin-1-deficient (KO) mice shares at least three salient features with changes elicited by bladder outflow obstruction. Whether contractile changes in the caveolin-1-deficient bladder are secondary to outflow obstruction or reflect a primary role of caveolae in detrusor signalling is not known with certainty as no mechanical study has focused on female mice.

Further questions regarding the detrusor phenotype remain unresolved. For instance, whereas genetic deletion of caveolin-1 impairs muscarinic contraction in the male mouse bladder (Lai *et al.*, 2004; 2007; Woodman *et al.*, 2004), pharmacological disruption of caveolae by cholesterol desorption has the opposite effect (Shakirova *et al.*, 2010). This may indicate that the bladder phenotype of caveolin-1-deficient mice is due to a developmental defect, rather than to a direct role of caveolae in signalling. Moreover, a generalized impairment of detrusor contractility with an unchanged bladder capacity is not reconcilable with normal maximal micturition pressure in caveolin-1-deficient male mice *in vivo* (Woodman *et al.*, 2004). The basis of the reduced release of acetylcholine in caveolin-1-deficient male urinary bladder (Lai *et al.*, 2004) also remains unexplained.

Our aim was to characterize detrusors from wild-type (WT) and caveolin-1-deficient (KO) female and male mice to determine if outflow obstruction caused by a hypertrophic prostate gland contributes to the detrusor phenotype. We also aimed to address the hypothesis that impaired neuroeffector transmission in the caveolin-1-deficient detrusor is due to altered innervation.

Methods

Animals

A series of 15 to 25 week-old caveolin-1-deficient (KO) and congenic age-matched C57Bl/6J WT female mice were used (Shakirova *et al.*, 2009). Forty-two KO mice, 50 WT mice and a smaller series (11 + 11 animals) of 40 week-old male WT/KO mice were used. Water bottles were weighed daily to assess diuresis. Mice were weighed after they had been killed by using CO_2. Bladders were excised and handled in cold Ca^{2+}-free HEPES-buffered Krebs (in mM: NaCl 135.5, KCl 5.9, $MgCl_2$ 1.2, glucose 11.6, HEPES 11.6, pH 7.4). Fat and membranes were removed and the emptied bladder was weighed. Procedures were approved by the Malmö/Lund Ethics Committee.

Length–tension relationships and force measurements

A 2 mm wide equatorial ring was prepared and opened and urothelium was removed. Six silk sutures were tied around the resulting strip. Length of the equatorial strip and lengths of individual preparations were determined. Preparations were mounted in quadruple myographs (three 610M, Danish Myo Technology, Aarhus, Denmark); 12 preparations from four mice (two WT and two KO) were run in parallel. Length–tension relationships were generated in a way that allows expression of length as equatorial bladder circumference (Uvelius, 2001). Preparations were equilibrated for 15 min in HEPES-buffered Krebs (2.5 mM Ca^{2+}, 37°C) at each length. They were then contracted with 60 mM K^+ (HK, 7 min), and relaxed in Ca^{2+}-free HEPES-buffered Krebs (10 min). We never stretched preparations more than one step beyond the length that was optimal for force development (L_0). Lengths were adjusted back to L_0 and strips were contracted with HK and relaxed for 25 min. Carbachol was added cumulatively. Following weighing, stress (force per cross-sectional area) was calculated by multiplying force (mN) with length (mm) and density (assumed to be 1.06 $mg \cdot mm^{-3}$), and dividing by weight (mg). Except for responses to ATP and electrical field stimulation (EFS), where peak force was measured, force was integrated during stimulation.

Electrical field stimulation (EFS)

Preparations were mounted as described (Shakirova *et al.*, 2010) and stretched to a basal tension of 8 mN ($\approx L_0$). Frequency–response curves were then generated (Shakirova *et al.*, 2010). Scopolamine (1 μM) was applied for 30 min prior to stimulation. α,β-methylene-ATP (10 μM) was added twice to desensitize purine receptors. Experiments were started and terminated by HK activation. Calcitonin gene-related peptide (CGRP) (100 nM, human αCGRP, Sigma Aldrich, St. Louis, MO, USA) and cocaine- and amphetamine-regulated transcript (CART) (10 or 30 nM, CART 61–102, a kind gift from Dr Lars Thim, Novo Nordisk A/S, Målöv, Denmark) were added during continuous EFS or prior to and during frequency–response curves.

Electron microscopy

Bladders (three WT and three KO) were filled with 0.3 mL fixative (2.5% glutaraldehyde in 150 mM sodium cacodylate buffer, pH 7.4) and immersed in fixative. After 30 min they were opened longitudinally, transferred to new fixative and maintained therein for 2 h. Mid-ventral segments were cut, post-fixed in 1% osmium tetroxide for 2 h, block-stained with uranyl acetate, dehydrated and embedded in Araldite. Semi-thin sections were stained with toluidine blue and areas were chosen and cut for electron microscopy using a JEOL JEM 1230 microscope (Joel, Tokyo, Japan) (Albinsson *et al.*, 2007).

Morphometry was performed using ImageJ (NIH, Bethesda, MD, USA).

Immunohistochemistry

Bladders were filled with 0.3 mL fixative [Stefanini's solution: 2% paraformaldehyde and 0.2% picric acid in 0.1 M phosphate-buffered saline (PBS), pH 7.2], immersed in fixative overnight (4°C), rinsed in Tyrode's solution containing 10% sucrose, mounted in Tissue-Tek (Sakura Finetek, Europe B.V., Zoeterwoude, the Netherlands) and frozen on dry ice. Ten micrometre thick equatorial sections were cut and thaw-mounted on slides. Sections were incubated overnight (4°C) with primary antibodies dissolved in phosphate-buffered saline (PBS, pH 7.2) containing 0.25% bovine serum albumin and 0.25% Triton X-100. The primary antibodies used were: rabbit monoclonal anti-Caveolin-1, D46G3, dilution 1:800 (Cell Signaling Technology – In Vitro Sweden AB, Stockholm, Sweden); rabbit polyclonal anti-vesicular acetylcholine transporter (VAChT), 9690, 1:1200 (EuroDiagnostica, Malmö, Sweden); rabbit polyclonal anti-synaptophysin, pSy38 (gift from Dr Wiedenmann, Heidelberg, Germany); goat polyclonal anti-CART, N-20, 1:800 (Santa Cruz Biotechnology Inc., Santa Cruz, CA, USA); guinea pig polyclonal anti-CGRP, M8513, 1:640 (EuroDiagnostica, Malmö, Sweden); rabbit polyclonal anti-neuropeptide K (NPK), NPK4, 1:600 (gift from Dr Theodorsson, Karolinska Institutet, Stockholm, Sweden). Sections were rinsed 2 × 10 min in PBS with 0.25% Triton X-100 and antibodies with specificity for rabbit, guinea pig, or goat IgG, coupled to Cy2 or Texas-Red (Jackson, West Grove, PA, USA), were applied for 1 h. Sections were mounted in PBS : glycerol (1:1) after rinsing. Specificity was tested using primary antisera pre-absorbed with excess amount of antigen or by omission of primary antibodies.

Paraffin sections were incubated in 0.3% hydrogen peroxide for 20 min at room temperature to block endogenous peroxidase activity. Sections were incubated for 1 h at room temperature with caveolin-1 antibody (1:3000) using the rabbit monoclonal antibody above. Horseradish peroxidase-conjugated anti-rabbit secondary antibody (K4002, Dako, Glostrup, Denmark) was added for 1 h at room temperature and immunoreactivity was detected with diaminobenzidine (Dako). Sections were counterstained with Mayer's haematoxylin.

For quantitative purposes, digital images (30 from each animal, n = 6) were acquired in an epi-fluorescence microscope (Olympus, Tokyo, Japan) using a digital camera (Nikon DS 2-MV, Nikon, Tokyo, Japan). Density was defined as ratio between the area of specific immunostaining and total bladder wall area using Biopix iQ software (BioPixAB, Göteborg, Sweden). Upper and lower thresholds of fluorescence intensity were set for each antibody.

Z-stacks were captured using an LSM 510 confocal microscope (Carl Zeiss, Oberkochen, Germany). For double staining, we used goat polyclonal anti-VAChT, SC7717, 1:100 (Santa Cruz Biotechnology); goat polyclonal anti-synaptophysin, SC7568, 1:100 (Santa Cruz Biotechnology); goat anti-CART, N-20, 1:800 (Santa Cruz Biotechnology); guinea pig anti-CGRP, 1:640 (EuroDiagnostica, Malmö, Sweden); and the anti-caveolin-1 antibody described above. Secondary antibodies (1:400) were coupled to Cy2 (rabbit), or Texas-Red (guinea pig or goat) (Jackson, West Grove, PA, USA).

Western blotting

Preparations (n = 10–18 mouse pairs) were frozen on the surface of a stainless steel press precooled in liquid N_2. After compression, tissue cakes were weighed and transferred to 1.5 mL Eppendorf tubes on dry ice. Samples were dissolved in 50 µL sodium dodecyl sulphate (SDS) sample buffer [62.5 mM Tris-HCl pH 6.8, 2% SDS (w/v), 10% (v/v) glycerol, 5% (v/v) mercaptoethanol] containing phosphatase and protease inhibitors (Bio-Rad, Hercules, CA, USA). Protein concentration was determined using the EZQ assay (R-33200, Molecular Probes, Invitrogen, San Diego, CA, USA). Twenty micrograms of protein was loaded in each well (5%, 7.5%, 12%, 15%, and gradient polyacrylamide gels, Bio-Rad). Proteins remaining on the gels were stained with Coomassie Blue (Biorad, Hercules, CA, USA). Nitrocellulose membranes (0.2 µm, Bio-Rad) were blocked in TBS-T [20 mM Tris-HCl, 0.5 M NaCl, 0.05% (v/v) Tween 20, pH 7.5] with 5% dry milk, washed in TBS-T, and incubated with primary antibodies against caveolin-1 (clone 2297, 1:1000; BD Biosciences, Stockholm, Sweden), M_3 muscarinic receptors (H-210, 1:500; Santa Cruz Biotechnology), phospholipase-$C_{\beta1}$ ($PLC_{\beta1}$) (610925, 1:500; BD Biosciences), pore-forming subunit of L-type Ca^{2+} channel ($Ca_V1.2$) (ACC-003, 1:200, Alomone Labs Ltd, Jerusalem, Israel), nitrotyrosine (AB5411, 1:1000; Millipore, Temecula, CA, USA), cavin-1 (611258, 1:500; BD Biosciences), and muscle-specific kinase (MuSK) (ab5619, 1:100; Abcam, Cambridge, UK). Horseradish peroxidase-conjugated secondary antibodies were used for detection (West Femto; Pierce, Rockford, IL, USA) in a Fluor-S™ MultiImager (Bio-Rad). Bands were normalized to total protein in the lane and then to the mean for all controls on the same membrane.

Quantitative RT-PCR

Bladders were frozen in liquid N_2 and homogenized in lysis buffer (Macherey-Nagel, Düren, Germany) using an Omni tissue homogenizor (Omni International, Kennesaw, GA, USA). RNA was isolated using Nucleospin® RNAII extraction kit (Macherey-Nagel). RNA concentration was determined in a ND-1000 spectrophotometer (Nanodrop Technologies Inc., Wilmington, DE, USA). cDNA was synthesized from 1 µg RNA with Precision qScript™ Reverse transcription kit (Primer Design, Southampton, UK). M_3 mRNA was analysed using SYBR green quantitative real-time PCR on M3000P (Stratagene, La Jolla, CA, USA). Amplification was performed as follows: 95°C for 10 min, 95°C 20 s, 60°C 1 min, for 45 cycles, followed by 1 min 95°C, 1 min 55°C, 30 s 95°C. Samples were run as triplicates in a volume of 20 µL. Expression levels were calculated using $2^{-\Delta\Delta Ct}$. M_3 levels were first normalized to glyceraldehyde 3-phosphate dehydrogenase (GAPDH) and then to the M_3 mRNA level in WT mice. The primer sequences were: 5′-ACTTACCGAGCCAAACGAACA-3′ (forward) and 5′-GCCCACAGGACAAAGGAGAT-3′ (reverse) (Primer Design). GAPDH primers [QuantiTect primer assay (Mn_Gapdh_3_SG)] were from Qiagen (Qiagen Inc., Valencia, CA, USA).

Statistics

The n-values refer to the number of mice. Means ± SEM are given. Student's unpaired t-test, one- or two-tailed as appropriate, was used to test for differences. $P < 0.05$ was considered

significant. Significance is indicated by asterisks: *$P < 0.05$, **$P < 0.01$ and ***$P < 0.001$.

Results

Body and bladder weights and diuresis in female caveolin-1-deficient mice

No differences in body weights (WT: 28.8 ± 0.3 g, KO: 27.7 ± 0.6 g, $n = 10$, $P > 0.05$) or urinary bladder weights (WT: 38.1 ± 1.9 mg, KO: 39.6 ± 4.2 mg, $n = 10$, $P > 0.05$) were noted, and no change in the bladder to body weight ratio was seen (1.32 ± 0.06 mg·g^{-1} vs. 1.43 ± 0.14 mg·g^{-1}, $P > 0.05$). The proportion of detrusor muscle relative to bladder wall thickness in toluidine blue-stained sections was not different between the two strains of mice (WT: 81 ± 2%, KO: 87 ± 2%, $n = 3$). However, 24 h drinking, an estimate of diuresis, was reduced in the KO group (WT: 0.21 ± 0.01 g·g^{-1} bodyweight, KO: 0.17 ± 0.01 g·g^{-1} bodyweight, $P < 0.05$, $n = 10$).

Caveolin-1 in the female detrusor and its intramural nerves

Immunohistochemical staining of the bladder for caveolin-1 disclosed labelling of muscle bundles in WT with little staining of the urothelium (Figure 1A). Similar to the muscle, fibroblasts in the submucosa were positive. No staining was detected in urinary bladders from KO mice (Figure 1A vs. B). In order to determine whether caveolin-1 is expressed in intramural bladder nerves, we used confocal imaging. Caveolin-1 was restricted to the muscle cell membrane and was often punctuated. Nerves, stained for either synaptophysin, VAChT, CGRP or CART, typically ran in parallel with the longitudinal axis of the muscle cells (Figure 1C–J). Little co-localization with caveolin-1 was seen.

Ultrastructure of the female detrusor muscle

Visualization of smooth muscle cells using electron microscopy did not disclose gross changes other than the lack of caveolae (Figure 2A vs. B). The plasma membrane of detrusor smooth muscle cells is partitioned into two domains: one harbouring dense bands and one in which caveolae reside. Ablation of caveolin-1 did not affect the proportion occupied by dense bands (52 ± 2% in WT vs. 59 ± 4% in KO, $n = 3$ for both). At high magnification (Figure 2C), caveolae (arrows) were seen in the dense band-free segments in WT (2.1 ± 0.2 caveolae per micrometre membrane, $n = 3$, 75–192 counted per specimen). Very few caveolae were found in KO (0.07 ± 0.03 caveolae per micrometre membrane, $n = 3$, $P < 0.001$ vs. WT, 2–11 counted per specimen, compare Figure 2D with Figure 2C). The diameter of 'open' caveolae in WT was 94 ± 2 nm ($n = 30$, i.e. 10 from each specimen). We could only identify nine open caveolae in the KO group. The diameter of these was 58 ± 3 nm ($P < 0.001$ vs. WT).

Vesicle-containing varicosities were identified in the muscle bundles. These were typically close to smooth muscle cells forming neuromuscular junctions which were similar in appearance in WT and KO (Figure 2E and F). The membrane opposite to nerve terminals often contained caveolae in WT cells.

Circumference–tension relationships

Circumference–tension relationships revealed active force (60 mM K^+, HK) to be reduced in KO at circumferences ranging between 1.5 and 2 cm (Figure 3A). Passive force (i.e. force under fully relaxing conditions) was not changed (Figure 3B). The optimum circumference for force generation (L_0) was not different in WT compared with KO (Figure 3C) whereas depolarization-induced stress (force per cross-sectional area in mN·mm^{-2}) at L_0 was reduced (Figure 3D).

The rate of contraction and relaxation on addition and withdrawal of HK revealed slower rates in both female and male KO mice (data not shown).

Bladder contraction elicited by the muscarinic receptor agonist carbachol

Concentration–response relationships for carbachol were generated at L_0 (Figure 4A shows original traces normalized to the initial peak of the HK response). Stress was reduced in KO compared with WT strips between 0.1 and 3 μM, whereas stress at supramaximal concentrations was unchanged (Figure 4B). When force was normalized to the HK response, an increase was observed in KO compared with WT at the three highest carbachol concentrations (Figure 4C).

The absence of a difference in stress at the highest carbachol concentrations in female caveolin-1-deficient detrusor contrasts with what has previously been reported for caveolin-1-deficient male detrusor. Similar to female KO detrusors, male KOs exhibited reduced stress at intermediate carbachol concentrations (see mean force ± SEM on application of 0.3 μM carbachol in six pairs of male mice in Figure 4D) without any reduction of the supramaximal response in our experiments (Figure 4E). The slightly greater impairment of stress at intermediate concentrations in male mice compared with female mice may relate to age because the male mice were older. Importantly, relative force was increased at the highest concentrations of carbachol in male mice (Figure 4F).

Bladder contraction in response to ATP

Concentration–response curves for ATP were generated in female detrusors and peak force expressed as stress and as a percentage of the HK response. ATP was applied at a single concentration followed by washing and a resting period of 15 min before the concentration was stepped up. Figure 5A shows the effect of 1 mM ATP. Summarized data showed stress to be reduced in KO compared with WT strips at concentrations below 3 mM (Figure 5B). Relative force was similarly reduced at low concentrations of ATP (Figure 5C). At the end of these experiments, we added the muscarinic receptor antagonist scopolamine (1 μM) and α,β-methylene-ATP (10 μM) to block muscarinic receptors and desensitize purine receptors. The integrated HK stress was also reduced in KO compared with WT strips under these conditions (Figure 5D).

Neuroeffector transmission

Intramural bladder nerves were activated using EFS. EFS-induced contractions were slightly reduced between 1–20 Hz whereas the peak EFS-induced contractions were similar and approached 300% of the integrated HK response in KO versus WT bladders (Figure 6A and B). After scopolamine addition,

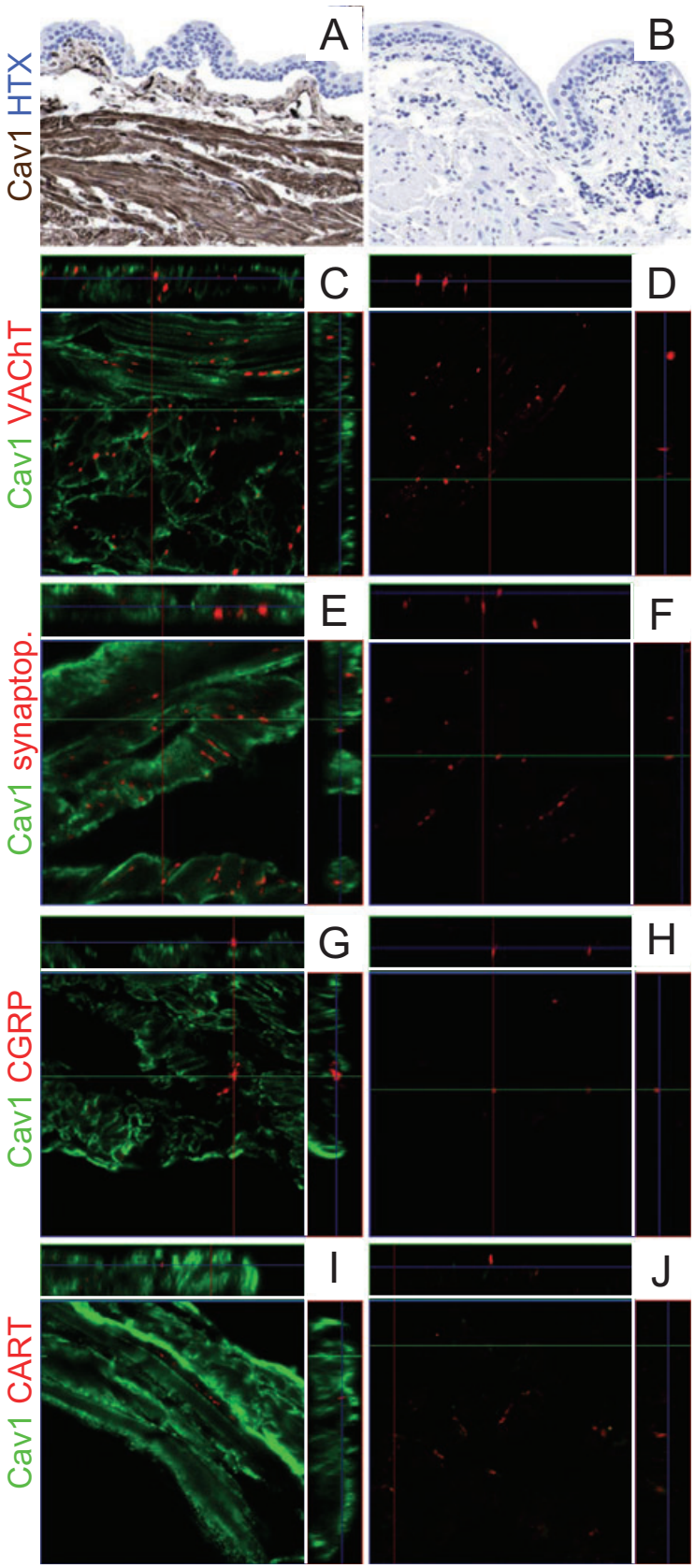
A
B
Cav1 HTX
C
D
Cav1 VAChT
E
F
Cav1 synaptop.
G
H
Cav1 CGRP
I
J
Cav1 CART

Figure 1

Staining for caveolin-1 (Cav1) and neural markers in the female urinary bladder (wild-type: A, C, E, G, I; KO: B, D, F, H, J). In (A) and (B) (590 μm × 440 μm) brown horseradish peroxidase reaction product shows caveolin-1-immunoreactivity, and blue shows counterstaining with Mayer's haematoxylin (HTX). (C–J) *Z*-stacks of caveolin-1 (green) and four neural markers (all red) as follows: vesicular acetylcholine transporter (VAChT), synaptophysin (synaptop.), calcitonin gene-related product (CGRP) and cocaine- and amphetamine-regulated transcript (CART). *Z*-stacks are compiled of 20 confocal images 1 μm apart. The main images show the *z*-plane (92 μm × 92 μm) whereas strips above and to the right show *x*- and *y*-planes (both 20 μm × 92 μm) at the green and red lines in the *z*-plane. Colocalization appears in yellow.

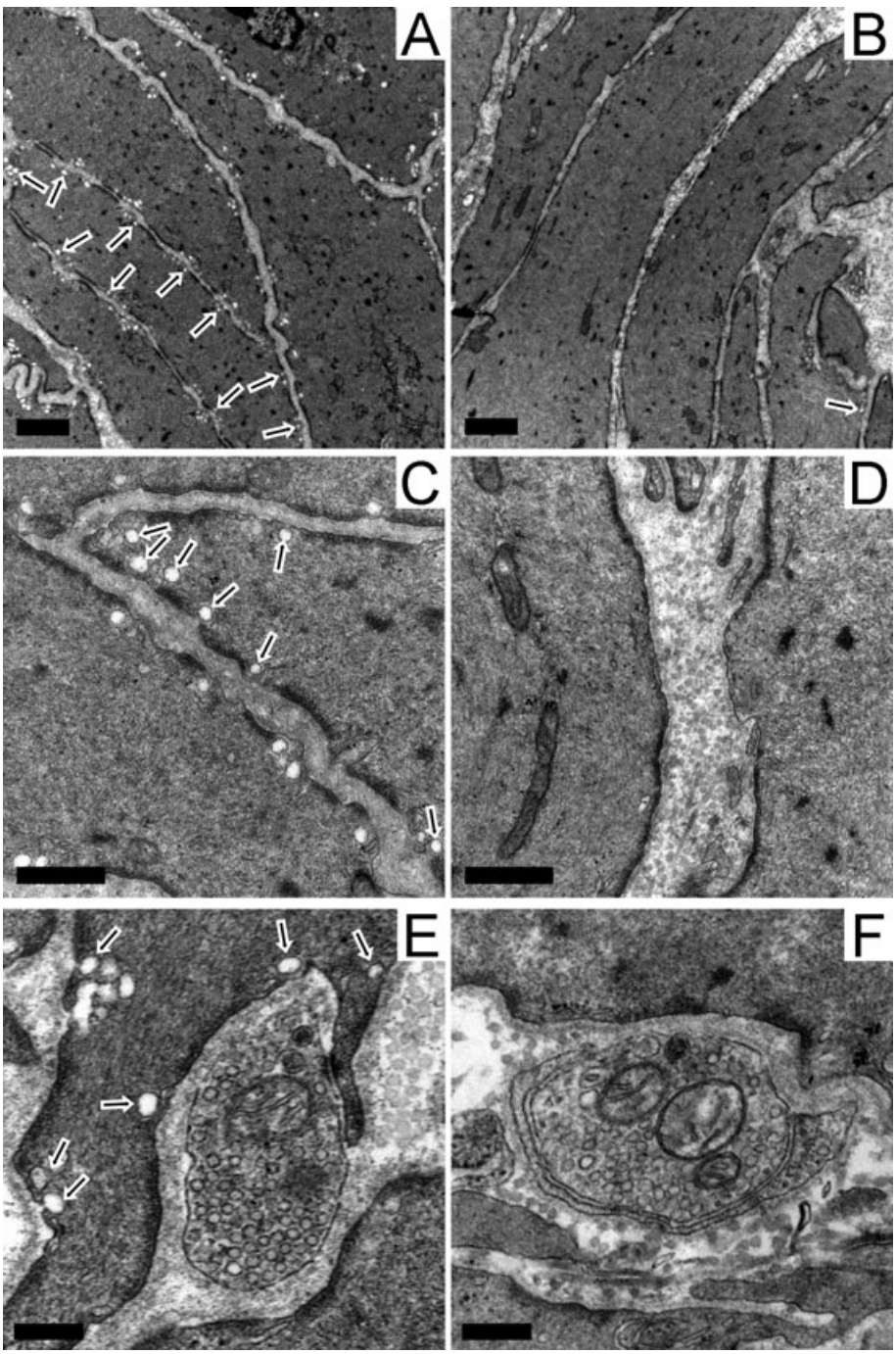

Figure 2

Visualization of smooth muscle cells (A–D) and nerve terminals (E and F) in female wild-type (A, C, E) and KO (B, D, F) detrusor by electron microscopy. Scale bars represent 1 μm (A and B), 0.5 μm (C and D) and 300 nm (E and F). Representative caveolae are highlighted with arrows (A–C and E). (E and F) Nerve terminals in wild-type and KO respectively.

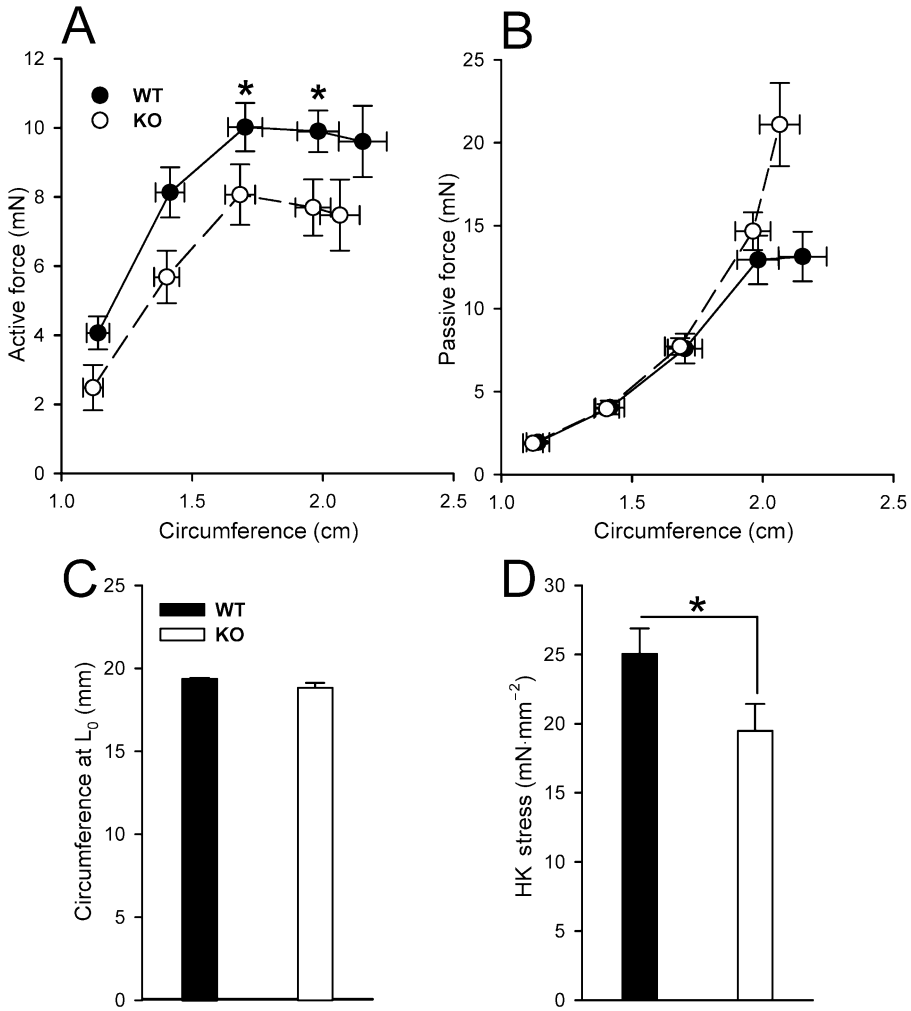

Figure 3

Active (A) and passive (B) force plotted as a function of circumference in wild-type and KO female bladder strips. The optimum circumference for force development (L_0) is shown in (C) and depolarization-induced force at L_0 is shown in (D) (n = 10 mice of each genotype).

the EFS-induced contraction was reduced by about half in WT strips and less in KO strips (Figure 6A and B). Desensitization of purine receptors using α,β-methylene-ATP in the presence of scopolamine eliminated the remaining EFS-induced contraction in both WT and KO (Figure 6A and B). We plotted the scopolamine-dependent part of the EFS-induced contraction to obtain a quantitative expression of the cholinergic component. The cholinergic component was reduced in the absence of caveolin-1 at frequencies between 1 and 20 Hz (Figure 6C). These findings indicate the presence of a defect in cholinergic neuroeffector transmission in caveolin-1-deficient female bladders because contraction in response to exogenously added carbachol was unchanged or increased, depending on concentration, when expressed relative to HK (cf. Figure 4C). The purinergic (α,β-methylene-ATP-sensitive) component of activation was not different (not shown).

Density of neuronal profiles

We hypothesized that the neurotransmission defect might be due to reduced innervation of the bladder and therefore quantified staining densities for VAChT and synaptophysin. No difference in the relative positive area was found for synaptophysin (Synap.) or VAChT (Figure 6D). We therefore also examined CART, CGRP and NPK, which mark distinct neuronal populations, to get a more comprehensive picture of the pattern of innervation. The relative area of CGRP and CART staining was reduced in KO bladders.

Effect of CGRP and CART on EFS-induced contraction in the mouse bladder

To determine whether a reduced density of CGRP- and CART-positive nerves might contribute to impaired cholinergic neurotransmission, frequency–response curves were generated in the presence and absence of these peptides. CGRP (100 nM) inhibited EFS-induced twitches in 3/8 WT bladder preparations (Figure 7A shows an example where inhibition was seen). The effect was rapid and had a magnitude of ~10% of the total response. When we plotted the scopolamine-sensitive component of activation in the entire material (Figure 7C) no effect was seen. CART (10 nM) was without

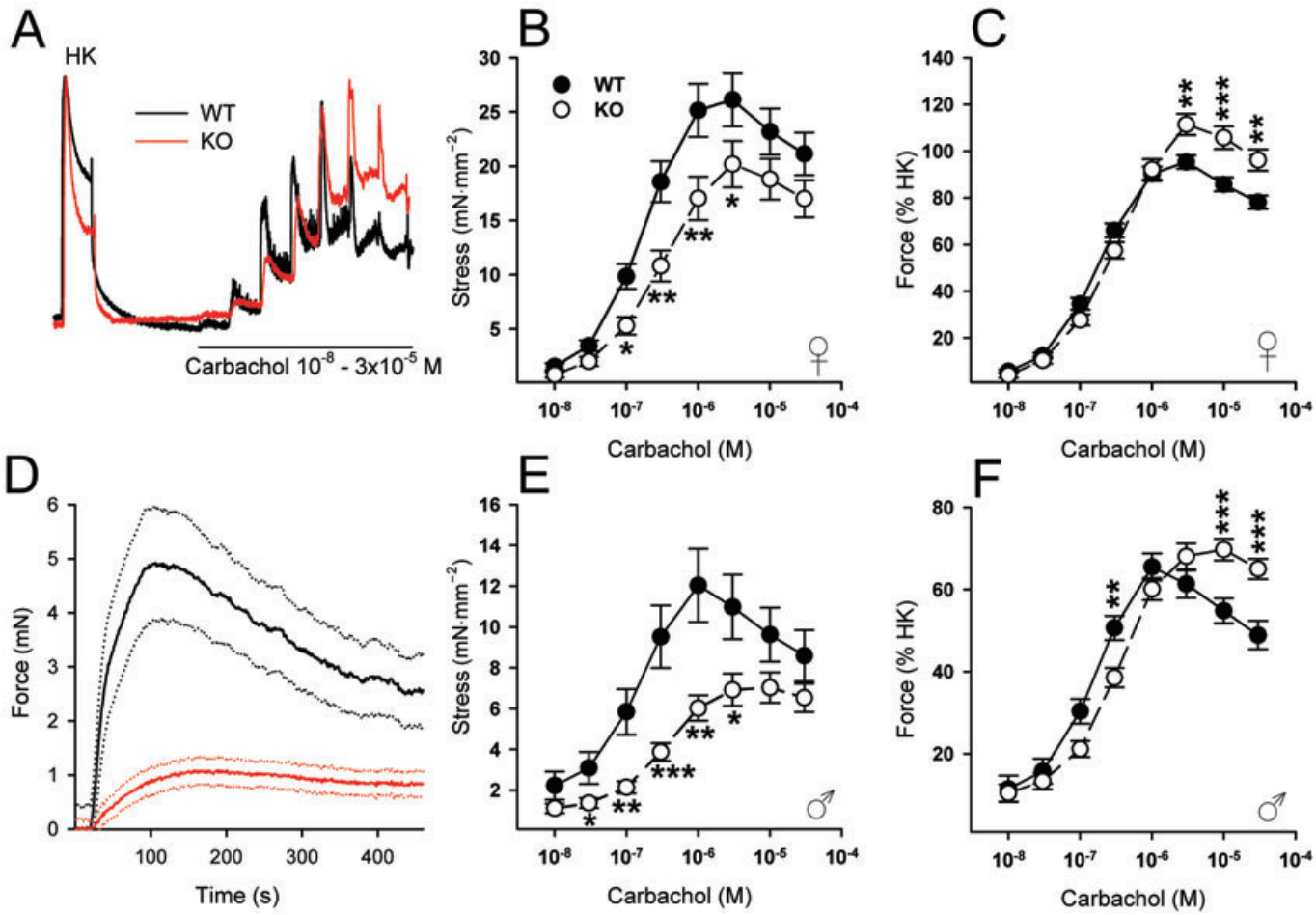

Figure 4

Force traces (A) depicting concentration–response curves for carbachol at L_0 in wild-type (WT) and KO female detrusors. Force was normalized to the peak contraction with 60 mM K^+ (HK) in these traces. Stress (B) in mN per cross-sectional area (n = 10 mice of each genotype) and contraction normalized to HK (C, n = 10 mice of each genotype) is shown for WT and KO. (D) Mean force (±SEM, dotted lines) following application of 0.3 μM carbachol (at 20 s) in WT and KO (red) male bladders (n = 6). (E and F) Concentration–response curves for carbachol in males with stress (E) and force expressed as a percentage of the initial HK response (F) on the y-axis (n = 6).

effect (unchanged twitch amplitude in 8/8 preparations, Figure 7B). Moreover, CART had no effect on the cholinergic component of activation (Figure 7D).

Tyrosine nitration and expression of signalling and scaffolding proteins

Increased activity of endothelial nitric oxide synthase is considered to underlie many phenotypes in caveolin-1-deficient mice. In the lung, this leads to changes in tyrosine nitration. To determine if such a mechanism could contribute to the biomechanical changes in the caveolin-1-deficient urinary bladder, we performed Western blotting for nitrated tyrosine. Lung and skeletal muscle lysates were included as positive controls. The pattern of tyrosine nitrated bands in lung and skeletal muscle was reminiscent of that obtained in previous studies, with two major bands at ~110 kDa and ~70 kDa (Figure 8A). The major tyrosine nitrated species in bladder migrated at ~32 kDa, but bands at ~70 kDa and ~110 kDa were clearly visible. No difference in tyrosine nitration of the 32 kDa band was found between WT and KO bladders (Figure 8B).

We next blotted for caveolin-1, cavin-1, $Ca_V1.2$, $PLC_{\beta1}$, M_3 muscarinic receptors and MuSK to better understand the functional changes observed. Caveolin-1 was absent in KO lysates as expected (Figure 8C). Two (or three) cavin-1 bands were detected in WT lysates whereas one major cavin-1-band, migrating slightly faster than the major WT band, was seen in KO lysates (Figure 8D). The pore-forming subunit, $Ca_V1.2$, of the L-type Ca^{2+} channel was unchanged (Figure 8E) as was $PLC_{\beta1}$ (Figure 8F). An increase in M_3 was seen in KO bladders (Figure 8G). We performed quantitative real-time PCR for M_3 in a separate series to corroborate up-regulation of M_3. This confirmed an increased M_3 expression in caveolin-1-deficient detrusor (Figure 8H). MuSK is tyrosine kinase receptor critical for the development of neuromuscular junctions. A single MuSK band of the expected molecular weight was observed in WT bladder lysates

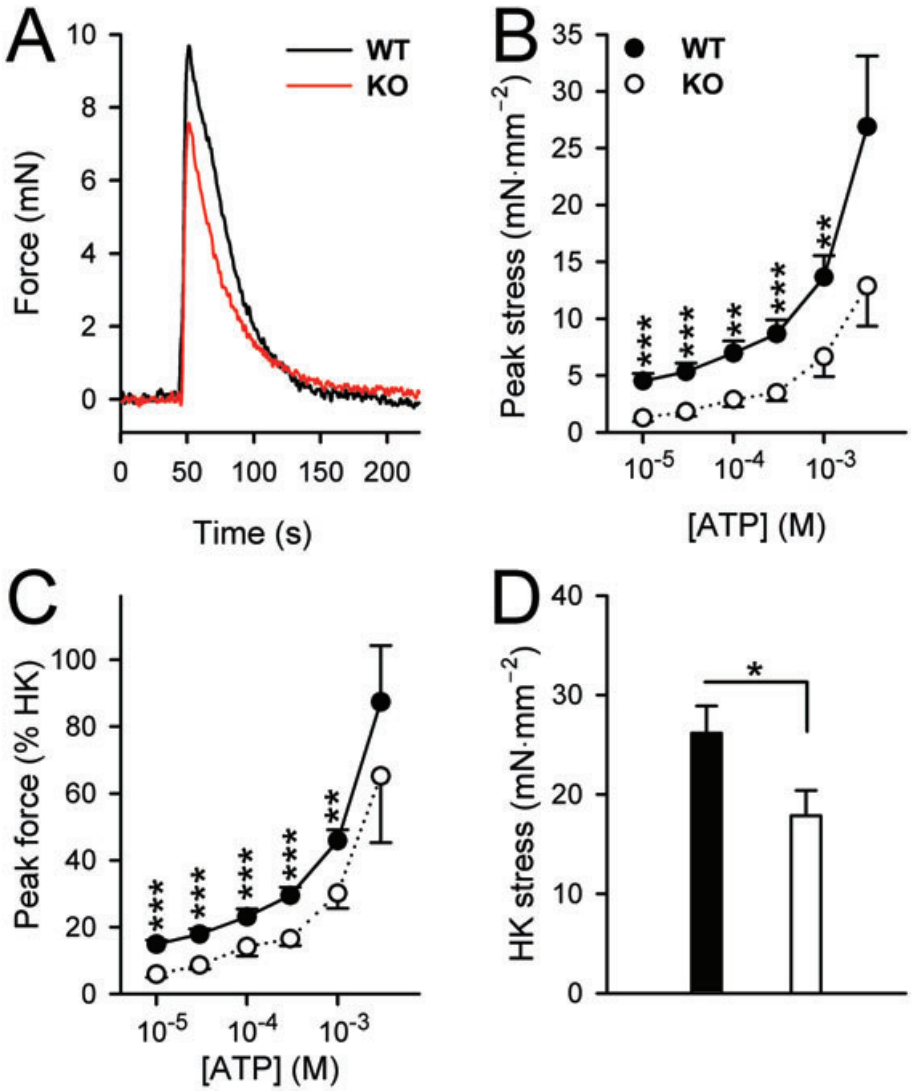

Figure 5

(A) Force in wild-type (WT) and KO detrusor preparations on application of 1 mM ATP. (B and C) Concentration–response curves for ATP with stress (B) and relative force (C) on the *y*-axes. (D) Mean force during stimulation with 60 mM K^+, equivalent to data in Figure 3D, but after desensitization of purine receptors with α,β-methylene-ATP (10 μM) and in the presence of the muscarinic receptor antagonist scopolamine (1 μM).

(Figure 8I). A reduction of MuSK was seen in KO detrusor lysates (Figure 8I and J).

Discussion

Genetic ablation of caveolae in the female detrusor is demonstrated here to be associated with substantial functional changes. Previous studies have focused on male mice, which may have prostate hypertrophy (Woodman *et al.*, 2004). Outlet obstruction such as that resulting from prostate hypertrophy is known to cause bladder growth, partial denervation and impaired muscarinic activation (Saito *et al.*, 1993; Andersson, 2003), that is changes reminiscent of those reported for male caveolin-1-deficient bladders. Our present findings in female mice thus rule out prostate hypertrophy as a critical contributing factor to the bladder phenotype. We propose that increased relative carbachol contraction at supramaximal concentrations is due to up-regulation of M_3 receptors, and that it represents an element of what is referred to as denervation supersensitivity (Emmelin, 1952). Denervation of the rat urinary bladder increases both the efficacy and potency for carbachol (Persson *et al.*, 1998). Partial loss of cholinergic neuroeffector transmission, that is functional denervation, combined with a primary deficit in contractile signalling in the detrusor is envisaged to underlie the complex changes in cholinergic activation seen here.

A cholinergic neuroeffector transmission defect in caveolin-1-deficient urinary bladder was first identified in male mice by Lai *et al.* (2004). It was found that the release of acetylcholine was reduced, and it was speculated that caveolin-1 plays a role in the exocytotic machinery. This

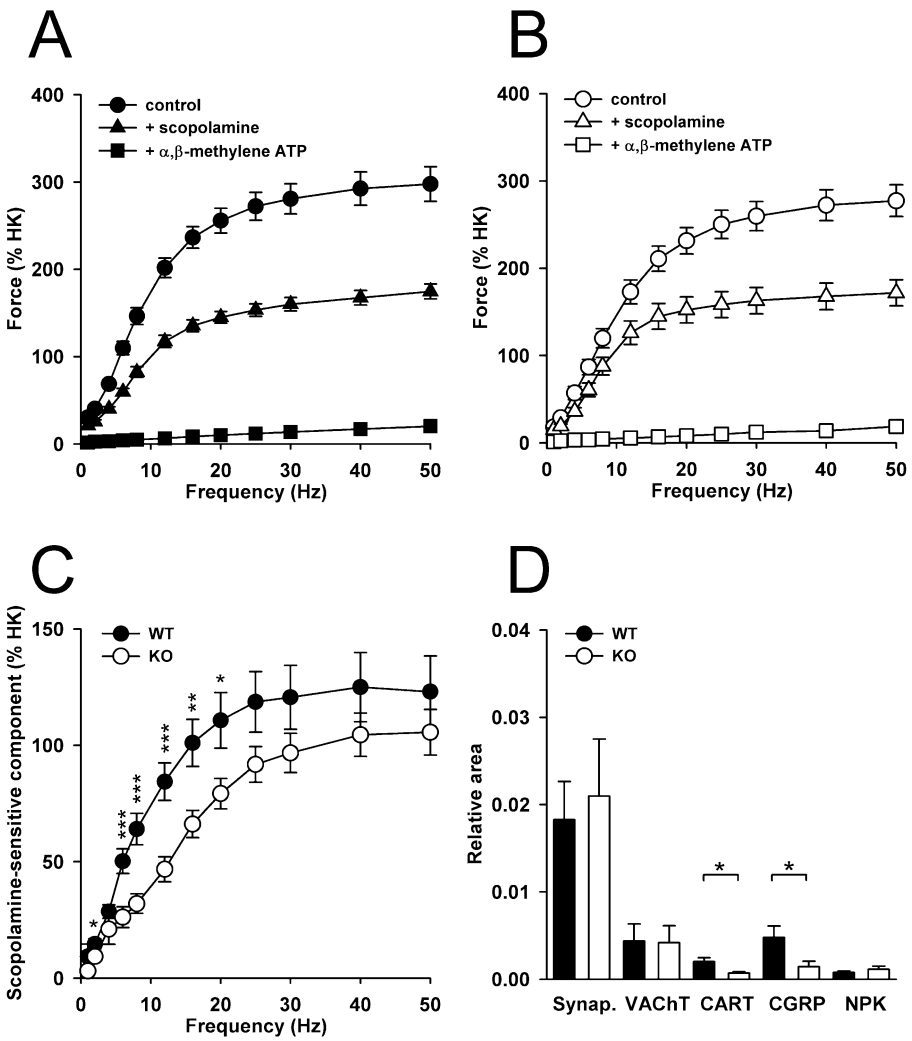

Figure 6

Contractions in response to electrical field stimulation (EFS) as a function of stimulation frequency in female wild-type (WT) (A) and KO (B) detrusors under control conditions, after pre-incubation with, and in the presence of, 1 μM scopolamine, and after prior desensitization of purine receptors using α,β-methylene-ATP (10 μM) and the presence of scopolamine. The scopolamine-sensitive (i.e. cholinergic) component of EFS-induced contraction (C) was derived by subtracting force in the presence of scopolamine from force in control conditions in WT and KO. In (D) the relative area of bladder neurones positive for synaptophysin (Synap.), vesicular acetylcholine transporter (VAChT), cocaine- and amphetamine-regulated transcript (CART), calcitonin gene-related peptide (CGRP) and neuropeptide K (NPK) is shown (n = 6).

speculation was based on the formation of a SNAP25-caveolin-1 complex after incubation of hippocampal slices with 4-aminopyridine (Braun and Madison, 2000). However, that complex was most abundant when synaptic transmission was depressed, undermining the notion that caveolin-1 facilitates the release of synaptic vesicles. Cultured sensory neurones and PC12 cells express caveolin-1 (Galbiati *et al.*, 1998), as do cultured hippocampal neurones (Braun and Madison, 2000). Our data however reveal that caveolin-1 expression in bladder axons and terminals *in situ* is low, if at all present, in comparison with smooth muscle. This does not rule out the presence of caveolin-1 in the somata of these neurones, but it provides a second argument against a direct facilitating role of caveolin-1 in vesicle release. Moreover, we did not find evidence for an altered density of cholinergic neurones in the bladder.

The neuropeptide CART has been identified in detrusor ganglia of newborn rats, and its localization changed during development, such that in adult animals it was found in tyrosine hydroxylase-positive cells (Zvarova and Vizzard, 2005). This suggests postganglionic neurones of the sympathetic nervous system as its location. CGRP marks sensory neurones (Gibson *et al.*, 1984). As indicated above, sensory and sympathetic neurones (PC12 cells) express caveolin-1 under some conditions (Galbiati *et al.*, 1998) and its loss from these neurones could affect growth or differentiation, explaining their reduced density.

Calcitonin gene-related peptide impairs EFS-induced detrusor contractions in many species (e.g. Giuliani *et al.*, 2001), and a similar effect was detected here in mouse. Reduced release of CGRP therefore does not explain the reduction of the muscarinic component of EFS-induced

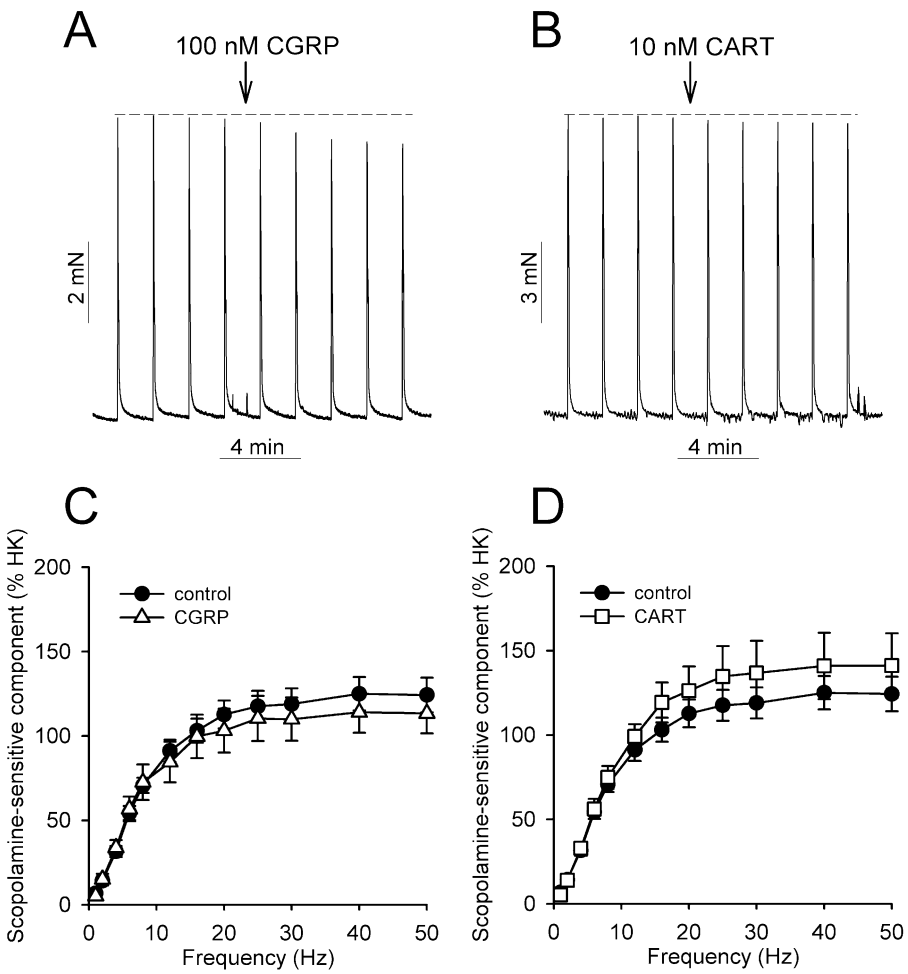

Figure 7

Addition of calcitonin gene-related peptide (CGRP) (A) and cocaine- and amphetamine-regulated transcript (CART) (B) to wild-type detrusors during electrical field stimulation (20 Hz, 5 s, every 2 min). (C and D) The cholinergic component of activation (derived as in Figure 6A–C) in the presence of 100 nM CGRP (C) and 10 nM CART (D).

activation. The loss of CGRP-positive neurones would rather be predicted to increase electrically-induced twitches. However, the altered density of CGRP-positive neurones may affect important sensory functions in the bladder. Because CART had little effect on EFS-induced contraction, the reduced density of CART-positive neurones also cannot explain the cholinergic neuroeffector transmission defect in caveolin-1-deficient bladder.

Muscle-specific kinase is a tyrosine kinase receptor expressed by myotubes (Valenzuela *et al.*, 1995). MuSK is activated by the glycoprotein Agrin (Glass *et al.*, 1996), which is released from motor neurones. MuSK plays a critical role in formation of neuromuscular junctions, affecting both pre- and postsynaptic differentiation (DeChiara *et al.*, 1996). It was recently demonstrated that caveolin-3 plays an important role in MuSK signalling (Hezel *et al.*, 2010). Further, evidence has been presented that Agrin is important for synaptic development in the autonomic nervous system (Gingras *et al.*, 2007), and Agrin is indeed expressed by cholinergic neurones in the urinary bladder (Gingras *et al.*, 2005). We now extend these findings by showing that MuSK is expressed in the urinary bladder and that its expression is reduced in the absence of caveolin-1, correlating with impaired cholinergic neurotransmission. Nerve terminals did however have the same general appearance as that described by Gabella (1995).

Clear-cut and important changes at the smooth muscle level were present in the caveolin-1-deficient female detrusor. Stress was reduced in response to low and intermediate concentrations of carbachol, low concentrations of ATP and depolarization. We therefore propose a general defect in contractility, involving cellular signalling, that is partly compensated for by up-regulation of M_3 receptors. The defective signalling mechanism remains to be established, but one possibility is that Ca^{2+}-sensitization is involved. Ca^{2+}-sensitization depends on the monomeric GTPase RhoA, and there is evidence that RhoA translocates to caveolae on activation with either agonist or KCl (Taggart *et al.*, 2000). Indeed, RhoA may be activated as a consequence of increased intracellular Ca^{2+} *per se* (Liu *et al.*, 2005), suggesting that

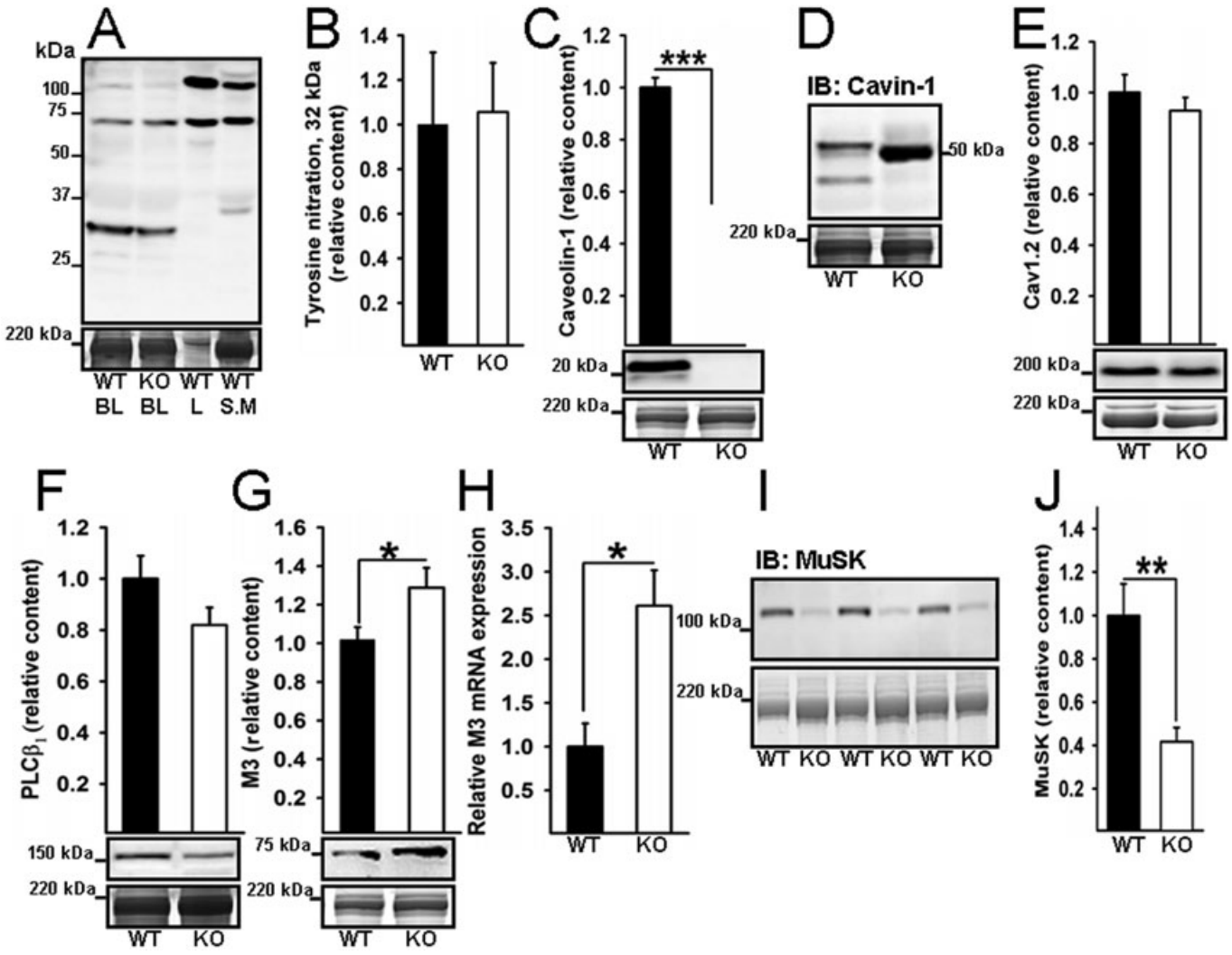

Figure 8

Immunoblots (IB) for nitrotyrosine (A; BL, bladder; L, lung; S.M, skeletal muscle; a summary of the data is shown in B), caveolin-1 (C), cavin-1 (D), $Ca_V1.2$ (E), phospholipases $C_{\beta1}$ ($PLC_{\beta1}$) (F) and M_3 muscarinic receptors (G). Quantitative real-time PCR for M_3 is shown in (H). (I) An IB for muscle-specific kinase (MuSK). Summarized data on MuSK expression are shown in (J). Below all immunoblots, sections of the gels, stained with Coomassie Blue after transfer (centred over the myosin band), are shown as a control for protein loading. When possible, membranes were cut in two to three pieces and incubated with different primary antibodies. Hence, some blots have the same loading control (e.g. C and G). For nitrotyrosine (A and B), we quantified the band at 32 kDa. The complex pattern of the bands seen with the cavin-1 antibody precluded quantification (n = 10–18 mouse pairs).

impaired translocation and activation of RhoA may well underlie a general defect. We can rule out altered nitric oxide synthase activity, because tyrosine nitration, previously demonstrated to be increased in lungs of caveolin-1-deficient mice (Zhao *et al.*, 2009), was unchanged. Reduced L-type Ca^{2+} currents can probably also be ruled out because available data for smooth muscle suggest similar L-type current densities in WT and caveolin-1-deficient smooth muscle cells (Cheng and Jaggar, 2006), and we found that expression of the pore-forming subunit of the L-type channel ($Ca_V1.2$) was unchanged.

M_3 receptors have been proposed to reside in and to depend on caveolae for signalling. For instance, fractionation and imaging as well as functional experiments supported localization of M_3 receptors in caveolae in canine and human airway smooth muscle cell (Gosens *et al.*, 2007). Similarly, in human bladder, M_3 receptors were clustered at the membrane, and chemical caveolae-ablation had a clear-cut effect on muscarinic contraction (Shakirova *et al.*, 2010). We did not examine the membrane distribution of M_3 in the mouse detrusor, but its localization in caveolae is not required to explain our present findings.

Maximal stress in male bladders was lower than in female bladders in the present set of experiments (compare Figure 4B and E). Several previous reports describe a drop in contractility of the detrusor with increasing age (Pfisterer *et al.*, 2006). This is in part due to changes in Ca^{2+} mobilization and intracellular signalling (Gomez-Pinilla *et al.*, 2008). Because our

male mice were 20 weeks older than our female mice, the differences in stress between female and male bladders in Figure 4B and E may be due to age rather than sex.

The present *in vitro* findings are more compatible with unchanged maximal micturition pressure in caveolin-1-deficient mice *in vivo* (Woodman *et al.*, 2004) than previous *in vitro* studies. Woodman *et al.* (2004) contracted bladder strips from 4 and 12 month-old caveolin-1-deficient male mice with carbachol in the concentration range 0.03–30 μM (i.e. approximately the same concentration range as used here) and found force to be reduced at all concentrations. Lai *et al.* (2004, 2007) used 1 and 10 μM carbachol and found contraction to be reduced at both concentrations. A potentially severe limitation of all previous studies, however, is that length–tension curves were not generated. Therefore, it is not known if the preparations were stretched to the optimum length for force development. In the present study we rigorously assessed L_0 in all preparations prior to the addition of carbachol and force was related to cross-sectional area throughout. Similarly sized KO bladders, with a 50–70% impairment of maximal muscarinic contraction (Lai *et al.*, 2004; 2007; Woodman *et al.*, 2004), unchanged or reduced purinergic contractility (Lai *et al.*, 2004, present study), and a cholinergic neuroeffector transmission defect (Lai *et al.*, 2004, present study), cannot generate similar maximal micturition pressures as WT bladders according to Laplace's law. Here we found that the contractility (stress) was unchanged at high concentrations of carbachol and a normalization of cholinergic transmission was observed at high stimulation frequencies. Our *in vitro* findings in the bladder thus predict a largely unchanged maximal micturition pressure *in vivo*.

We measured the quantity of water drunk by each group of mice in order to rule out a major increase in diuresis that would affect bladder structure and function. To our surprise, the volume drunk was slightly reduced in caveolin-1-deficient female mice. The drinking of water can only be equated with diuresis provided that metabolic rates and water loss via other routes are similar. Assuming this to be the case, our data indicate reduced diuresis in caveolin-1-deficient mice. A putative explanation is that caveolin-1 plays an inhibitory role in urea transport in the kidney (Feng *et al.*, 2009). The absence of caveolin-1 would thus be expected to allow for a more effective build up of an interstitial osmotic gradient. This would in turn improve water reabsorption and reduce diuresis. However, other mechanisms are also possible as caveolin-1 has been suggested to play additional roles in the kidney (Cao *et al.*, 2003).

Finally, caveolin-1, rather than caveolin-3, is responsible for the formation of the majority of caveolae in the female detrusor as reported for male mice (Woodman *et al.*, 2004). Rare examples of small (~60 nm) caveolae were found in bladders from caveolin-1 deficient mice that may represent caveolin-3-driven caveolae. The number of caveolae in caveolin-1-deficient detrusor corresponds to ~3% of the total number of caveolae in WT.

Conclusion

Genetic ablation of caveolae in female detrusor leads to mechanical changes akin to those in male caveolin-1-deficient mice, ruling out outlet obstruction as a contributing factor. Our data suggest that lack of caveolin-1 causes a general impairment of detrusor contractility that is partly compensated for by up-regulation of M_3 receptors. Lack of caveolin-1 also impairs cholinergic neuroeffector transmission. This is not associated with a reduced density of cholinergic nerves, but correlates with reduced expression of MuSK. Lack of caveolin-1 is, however, associated with reduced density of CGRP-positive nerves, of possible relevance for bladder sensory function.

Acknowledgements

The present study is supported by grants from the Swedish Research Council (K2009-65X-4955-01-3, 522-2008-4216, K2009-55X 21111-01-4), ALF, the Crafoord Foundation, the Royal Physiographic Society, Lars Hierta's Foundation, Greta and Johan Kock's Foundation, the Novo Nordisk Foundation, the Gyllenstiernska Krapperup, the Fredrik and Ingrid Thuring Foundation, the Magnus Bergwall Foundation, the Albert Påhlsson Foundation, The Swedish Society of Medicine and the Faculty of Medicine at Lund University. K. S. holds a Researcher position at the Swedish Research Council. We thank Doris Persson and Ann-Helén Thorén-Fischer for technical assistance.

Conflict of interest

None.

References

Absi M, Burnham MP, Weston AH, Harno E, Rogers M, Edwards G (2007). Effects of methyl beta-cyclodextrin on EDHF responses in pig and rat arteries; association between SK(Ca) channels and caveolin-rich domains. Br J Pharmacol 151: 332–340.

Albinsson S, Shakirova Y, Rippe A, Baumgarten M, Rosengren BI, Rippe C *et al.* (2007). Arterial remodeling and plasma volume expansion in caveolin-1-deficient mice. Am J Physiol Regul Integr Comp Physiol 293: R1222–R1231.

Andersson KE (2003). Storage and voiding symptoms: pathophysiologic aspects. Urology 62 (Suppl. 2): 3–10.

Babiychuk EB, Smith RD, Burdyga T, Babiychuk VS, Wray S, Draeger A (2004). Membrane cholesterol regulates smooth muscle phasic contraction. J Membr Biol 198: 95–101.

Bastiani M, Liu L, Hill MM, Jedrychowski MP, Nixon SJ, Lo HP *et al.* (2009). MURC/Cavin-4 and cavin family members form tissue-specific caveolar complexes. J Cell Biol 185: 1259–1273.

Braun JE, Madison DV (2000). A novel SNAP25-caveolin complex correlates with the onset of persistent synaptic potentiation. J Neurosci 20: 5997–6006.

Cao G, Yang G, Timme TL, Saika T, Truong LD, Satoh T *et al.* (2003). Disruption of the caveolin-1 gene impairs renal calcium reabsorption and leads to hypercalciuria and urolithiasis. Am J Pathol 162: 1241–1248.

Cheng X, Jaggar JH (2006). Genetic ablation of caveolin-1 modifies Ca^{2+} spark coupling in murine arterial smooth muscle cells. Am J Physiol Heart Circ Physiol 290: H2309–H2319.

Cohen AW, Hnasko R, Schubert W, Lisanti MP (2004). Role of caveolae and caveolins in health and disease. Physiol Rev 84: 1341–1379.

DeChiara TM, Bowen DC, Valenzuela DM, Simmons MV, Poueymirou WT, Thomas S *et al.* (1996). The receptor tyrosine kinase MuSK is required for neuromuscular junction formation *in vivo*. Cell 85: 501–512.

Emmelin N (1952). Paralytic secretion of saliva; an example of supersensitivity after denervation. Physiol Rev 32: 21–46.

Feng X, Huang H, Yang Y, Fröhlich O, Klein JD, Sands JM *et al.* (2009). Caveolin-1 directly interacts with UT-A1 urea transporter: the role of caveolae/lipid rafts in UT-A1 regulation at the cell membrane. Am J Physiol Renal Physiol 296: F1514–F1520.

Gabella G (1995). The structural relations between nerve fibres and muscle cells in the urinary bladder of the rat. J Neurocytol 24: 159–187.

Galbiati F, Volonte D, Gil O, Zanazzi G, Salzer JL, Sargiacomo M *et al.* (1998). Expression of caveolin-1 and -2 in differentiating PC12 cells and dorsal root ganglion neurons: caveolin-2 is up-regulated in response to cell injury. Proc Natl Acad Sci U S A 95: 10257–10262.

Gibson SJ, Polak JM, Bloom SR, Sabate IM, Mulderry PM, Ghatei MA *et al.* (1984). Calcitonin gene-related peptide immunoreactivity in the spinal cord of man and of eight other species. J Neurosci 4: 3101–3111.

Gingras J, Spicer J, Altares M, Zhu Q, Kuchel GA, Ferns M (2005). Agrin becomes concentrated at neuroeffector junctions in developing rodent urinary bladder. Cell Tissue Res 320: 115–125.

Gingras J, Rassadi S, Cooper E, Ferns M (2007). Synaptic transmission is impaired at neuronal autonomic synapses in agrin-null mice. Dev Neurobiol 67: 521–534.

Giuliani S, Santicioli P, Lippi A, Lecci A, Tramontana M, Maggi CA (2001). The role of sensory neuropeptides in motor innervation of the hamster isolated urinary bladder. Naunyn Schmiedebergs Arch Pharmacol 364: 242–248.

Glass DJ, Bowen DC, Stitt TN, Radziejewski C, Bruno J, Ryan TE *et al.* (1996). Agrin acts via a MuSK receptor complex. Cell 85: 513–523.

Gomez-Pinilla PJ, Gomez MF, Swärd K, Hedlund P, Hellstrand P, Camello PJ *et al.* (2008). Melatonin restores impaired contractility in aged guinea pig urinary bladder. J Pineal Res 44: 416–425.

Gosens R, Stelmack GL, Dueck G, Mutawe MM, Hinton M, McNeill KD *et al.* (2007). Caveolae facilitate muscarinic receptor-mediated intracellular Ca^{2+} mobilization and contraction in airway smooth muscle. Am J Physiol Lung Cell Mol Physiol 293: L1406–L1418.

Hezel M, de Groat WC, Galbiati F (2010). Caveolin-3 promotes nicotinic acetylcholine receptor clustering and regulates neuromuscular junction activity. Mol Biol Cell 21: 302–310.

Hill MM, Bastiani M, Luetterforst R, Kirkham M, Kirkham A, Nixon SJ *et al.* (2008). PTRF-Cavin, a conserved cytoplasmic protein required for caveola formation and function. Cell 132: 113–124.

Lai HH, Boone TB, Yang G, Smith CP, Kiss S, Thompson TC *et al.* (2004). Loss of caveolin-1 expression is associated with disruption of muscarinic cholinergic activities in the urinary bladder. Neurochem Int 45: 1185–1193.

Lai HH, Boone TB, Thompson TC, Smith CP, Somogyi GT (2007). Using caveolin-1 knockout mouse to study impaired detrusor contractility and disrupted muscarinic activity in the aging bladder. Urology 69: 407–411.

Lisanti MP, Scherer PE, Vidugiriene J, Tang Z, Hermanowski-Vosatka A, Tu YH *et al.* (1994a). Characterization of caveolin-rich membrane domains isolated from an endothelial-rich source: implications for human disease. J Cell Biol 126: 111–126.

Lisanti MP, Scherer PE, Tang Z, Sargiacomo M (1994b). Caveolae, caveolin and caveolin-rich membrane domains: a signalling hypothesis. Trends Cell Biol 4: 231–235.

Liu C, Zuo J, Pertens E, Helli PB, Janssen LJ (2005). Regulation of Rho/ROCK signaling in airway smooth muscle by membrane potential and $[Ca^{2+}]_i$. Am J Physiol Lung Cell Mol Physiol 289: L574–L582.

Liu J, Oh P, Horner T, Rogers RA, Schnitzer JE (1997). Organized endothelial cell surface signal transduction in caveolae distinct from glycosylphosphatidylinositol-anchored protein microdomains. J Biol Chem 272: 7211–7222.

Murakumo M, Ushiki T, Koyanagi T, Abe K (1993). Scanning electron microscopic studies of smooth muscle cells and their collagen fibrillar sheaths in empty, distended and contracted urinary bladders of the guinea pig. Arch Histol Cytol 56: 441–449.

Persson K, Alm P, Uvelius B, Andersson KE (1998). Nitrergic and cholinergic innervation of the rat lower urinary tract after pelvic ganglionectomy. Am J Physiol 274 (Pt 2):R389–R397.

Pfisterer MH, Griffiths DJ, Schaefer W, Resnick NM (2006). The effect of age on lower urinary tract function: a study in women. J Am Geriatr Soc 54: 405–412.

Rothberg KG, Heuser JE, Donzell WC, Ying YS, Glenney JR, Anderson RG (1992). Caveolin, a protein component of caveolae membrane coats. Cell 68: 673–682.

Saito M, Wein AJ, Levin RM (1993). Effect of partial outlet obstruction on contractility: comparison between severe and mild obstruction. Neurourol Urodyn 12: 573–583.

Shakirova Y, Hedlund P, Swärd K (2009). Impaired nerve-mediated relaxation of penile tissue from caveolin-1 deficient mice. Eur J Pharmacol 602: 399–405.

Shakirova Y, Mori M, Ekman M, Erjefält J, Uvelius B, Swärd K (2010). Human urinary bladder smooth muscle is dependent on membrane cholesterol for cholinergic activation. Eur J Pharmacol 634: 142–148.

Taggart MJ (2001). Smooth muscle excitation-contraction coupling: a role for caveolae and caveolins? News Physiol Sci 16: 61–65.

Taggart MJ, Leavis P, Feron O, Morgan KG (2000). Inhibition of PKCalpha and RhoA translocation in differentiated smooth muscle by a caveolin scaffolding domain peptide. Exp Cell Res 258: 72–81.

Uvelius B (2001). Length-tension relations of *in vitro* urinary bladder smooth muscle strips. J Pharmacol Toxicol Methods 45: 87–90.

Valenzuela DM, Stitt TN, DiStefano PS, Rojas E, Mattsson K, Compton DL *et al.* (1995). Receptor tyrosine kinase specific for the skeletal muscle lineage: expression in embryonic muscle, at the neuromuscular junction, and after injury. Neuron 15: 573–584.

Woodman SE, Cheung MW, Tarr M, North AC, Schubert W, Lagaud G *et al.* (2004). Urogenital alterations in aged male caveolin-1 knockout mice. J Urol 171 (Pt 1):950–957.

Zhao YY, Zhao YD, Mirza MK, Huang JH, Potula HH, Vogel SM *et al*. (2009). Persistent eNOS activation secondary to caveolin-1 deficiency induces pulmonary hypertension in mice and humans through PKG nitration. J Clin Invest 119: 2009–2018.

Zvarova K, Vizzard MA (2005). Distribution and fate of cocaine- and amphetamine-regulated transcript peptide (CARTp)-expressing cells in rat urinary bladder: a developmental study. J Comp Neurol 489: 501–517.